A Quantum Chemical Study of Bonding Interaction, Vibrational Frequencies, Force Constants, and Vibrational Coupling of Pyridine−M_n (M = Cu, Ag, Au; n = 2−4)

D. Y. Wu,*,†,§ M. Hayashi,‡ Y. J. Shiu,† K. K. Liang,† C. H. Chang,† Y. L. Yeh,† and S. H. Lin*,†

Institute of Atomic and Molecular Sciences, Academia Sinica, P.O. Box 23-166, Taipei, Taiwan 106, Republic of China, Center for Condensed Matter Sciences, National Taiwan University, 1 Roosevelt Rd., Sec. 4, Taipei, Taiwan 10764, Republic of China, and Department of Chemistry Chemistry and State Key Laboratory for Physical Chemistry of Solid Surfaces, Xiamen University, Xiamen, 361005 Fujian, China

Received: April 9, 2003; In Final Form: July 22, 2003

The binding interactions between the pyridine and small noble metal clusters in different sizes (n = 2−4) have been investigated by using quantum chemical methods. The binding energies of Py−M_2 complexes are obtained at the levels of the Hartree−Fock method (HF), the second-order Møller−Plesset perturbation theory (MP2), the local density functional method (SVWN), the nonlocal density functional method (BLYP, BPW91, G96LYP, G96PW91), and the hybrid density functional method (B3LYP and B3PW91). All calculated results show that the bonding is stronger in pyridine/copper and pyridine/gold than that in pyridine/silver. The bonding mechanism is explored in terms of the bonding molecular orbital properties. The donation interaction of the lone-pair electrons on nitrogen of the pyridine molecule to the unoccupied orbital of each metal cluster plays an important role. The force constants of the internal coordinates of interests are presented. The vibrational frequency shift has been analyzed on the basis of the coupling between the internal vibrational modes of pyridine and the nitrogen−metal stretching modes as well as the metal−metal stretching modes. For low-frequency Raman spectra of pyridine−small silver cluster complexes, we propose a new assignment to the N−Ag and Ag−Ag stretching vibrations. The calculated infrared intensities of vibrational modes are compared with the experimental spectra.

Introduction

The binding of a chromophore molecule to metal is an important issue in metal cluster chemistry, surface chemistry, and molecular electronics research, as in these aspects one often wishes to understand the structural properties, electronic properties, and vibrational spectroscopic properties.[1,2] An important aromatic molecule, pyridine (Py), has been extensively studied by numerous spectroscopic methods such as infrared spectroscopy and Raman spectroscopy in the gas,[3−5] liquid,[5−7] and metal interfaces.[8−25] The shift of vibrational frequencies and the change of the spectral intensities depend on the bonding interaction and the metal properties.

Because one CH of benzene is replaced by a nitrogen atom, there are two possible forms of pyridine bonding to metal atoms: N-end lone-paired σ-orbital bonding and π-orbital bonding. Numerous observed spectra of infrared and Raman spectroscopy have indicated that the chemisorption state of the pyridine molecule on the noble metal surfaces has the upright or slightly tilted configuration through the N-end bonding to metal atoms preferred in the case of the high coverage.[9−14,18,20−23] The bonding of pyridine N-end to metal surfaces was also confirmed by near-edge X-ray absorption fine-structure measurement for pyridine adsorbed on Ag(111)[26] and photoelectron diffraction experiment for pyridine on Cu(110).[27] Another kind of evidence for supporting the binding orientation is that low-frequency bands are often observed at about 235 cm^{-1} for pyridine interacting with silver,[11a,13,14,20] 240 cm^{-1} for copper,[20,28] and 260 cm^{-1} for gold in surface-enhanced Raman spectra (SERS).[10a,20,28] These bands have been assigned to the N−Ag stretch, the N−Cu stretch, and the N−Au stretch, respectively.

The vibrational frequency of the N−M (M = Cu, Ag, and Au) stretch has been explored theoretically. In the early modeling studies, Lombardi et al. adopted a force constant of the N−Ag bond to be about 1.5 mdyn/Å for estimating the frequency of the N−Ag stretching mode.[11a] They obtained the calculated vibrational frequencies of the N−Ag stretches in a good agreement with the experimental data for pyridine derivatives adsorbed on silver surfaces. On the basis of the calculated results, they suggested that one can distinguish the adsorption state between an adsorbed molecule bound directly to a metal surface as opposed to one bonded to a metal adatom which is itself bound to a metal surface. Moskovits studied the relationship by assuming the force constant of the N−Ag stretch to be 1.0 mdyn/ Å.[29] One model is Py−Ag−Ag; another model is a case that pyridine is directly bound to a silver tetramer, which configuration is similar to the form of pyridine adsorbed at the fourfold hollow site on a Ag(100) surface. Recently, Mizutani and Ushioda analyzed the vibrational frequency shift of internal modes of pyridine adsorbed on the rough silver surface.[30] They also calculated the vibrational frequency of the molecule−metal bond only to be 106.4 cm^{-1} by using the force constant of 0.57 mdyn/Å. They interpreted that the discrepancy between the

* Address correspondence to this author.
† Academia Sinica.
‡ National Taiwan University.
§ Xiamen University.

10.1021/jp034951l CCC: $25.00
Published on Web 10/17/2003

theory and experiment was possibly due to the lateral interactions between adsorbed pyridine molecules. More recently, a series of theoretical studies have been carried out on the systems of the pyridine interacting with noble metals and transition metals.[11d,31,32] The calculated results indicate that for neutral Py−M (M = Cu, Ag, Au) complexes the vibrational frequencies of the N−M stretches are obviously lower than the experimental values. A comparison of the binding energies of pyridine with small metal cluster indicates that the N−M bond is stronger in Py−M_2, Py−M_3, and Py−M_4 than that in Py−M.[32] Also, the vibrational frequencies of the N−M stretches increase with the binding energy, but these vibrational frequencies are still small.

In this paper, we will provide the further results on the bonding interaction and vibrational spectral properties of neutral pyridine−metal complexes. We investigate the interaction between pyridine and metal dimers (Cu, Ag, and Au) at various theoretical levels, including the Hartree−Fock method (HF), the second-order Møller−Plesset perturbation method (MP2), local (SVWN) and nonlocal density functional theoretical (DFT) method (SVWN, BLYP, BPW91, G96LYP, G96PW91), and hybrid DFT methods (B3LYP and B3PW91). All the calculated results show that the bonding is stronger in pyridine/copper and pyridine/gold than that in pyridine/silver. On the basis of the molecular orbital theory, we compare the present result with the previous results. Our present result will show that the hybrid DFT method provides the best result to the present systems of interest. Our result on the infrared intensities of internal modes of pyridine indicates that the bonding interaction affects the relative intensity of the different modes. Finally, the vibrational frequency shift is discussed on the basis of the coupling between vibrational modes. The analysis of the vibrational coupling of the various modes with the N−M stretches is helpful to understand the interaction between pyridine and metals in terms of the experimental spectra.

Computational Details

We consider model complexes consisting of a pyridine molecule and metal clusters of copper, silver, and gold in different sizes. We assume that each complex has a structure in which the N-end of the pyridine molecule approaches a metal atom of the metal cluster with C_{2v} point group symmetry, as we adopted in the previous calculations.[31,32] In this case, the molecular orbitals and vibrational modes of the pyridine molecule in each complex can keep the same symmetries as a free pyridine molecule. The configurations of these pyridine−metal cluster complexes are shown in Figure 1. Since the ground state of free pyridine is $^1A_1$, the group states for the complexes are $^2A_1$ for Py−M, $^1A_1$ for Py−M_2 and Pyr−M_4, as well as $^2B_2$ for Py−M_3.

For checking the validity of the theoretical methods, we carried out the fully geometric optimization of the ground states for Py−M_2 (Cu, Ag, Au) by using HF, MP2, SVWN, BLYP, BPW91, G96LYP, G96PW91, B3LYP, and B3PW91 methods in Gaussian 98.[33] The standard relativistic effective small core potential LanL2DZ is used to describe the inner-shell electrons for metal atoms.[34] The corresponding basis set Lanl2DZ is used to treat explicitly 19 electrons in the outer valence-shell orbitals of each atom.[34] The basis set for the atoms in pyridine is of the three-zeta quality, 6-311+G(d, p). This basis set with the B3LYP method can reproduce quite well experimental geometric structures and frequencies of the isolated pyridine molecule.[31] The binding energy (BE) of Py−M_2 complexes is calculated in terms of the expression

$$\mathrm{BE} = -(E_{\mathrm{Py-M_2}} - E_{\mathrm{Py}} - E_{\mathrm{M_2}}) \qquad (1)$$

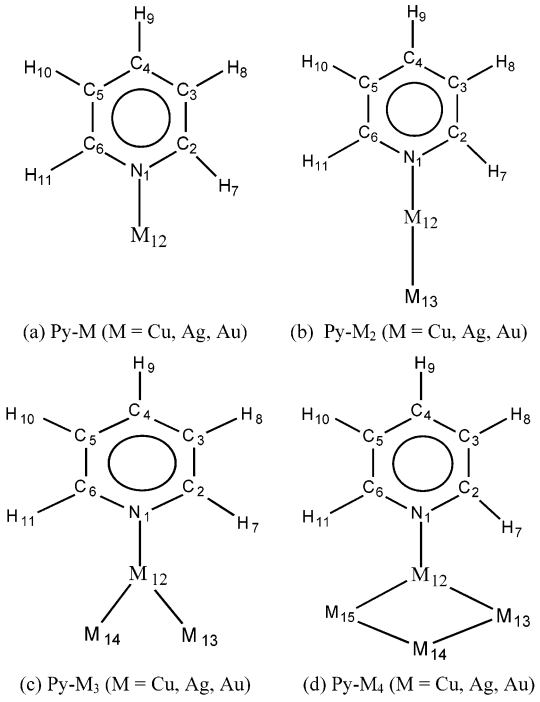

Figure 1. Structures of Py−M_n (M = Cu, Ag, and Au; n = 1−4).

where $E_{\mathrm{Py-M_2}}$, $E_{\mathrm{M_2}}$, and E_{Py} represent energies of Py−M_2, M_2, and the pyridine molecule obtained by using the methods as mentioned above.

The local symmetric coordinates for the pyridine−metal complexes in the normal-mode analysis are defined using the method given by Pulay et al.[35,36] For Py−M, the coordinates involved in the metal atom are the same as the definition in the previous paper.[31] For Py−M_2, there are six new symmetric coordinates, for example, both stretches of the N−M and M−M bonds (A_1), the in-plane (B_2) and out-of-plane bends (B_1) of the N−M bond, two linear bending coordinates, that is, the out-of-plane (B_1) and the out-of-plane (A_2) bends of the N−M−M moiety. For Py−M_3 and Py−M_4, the new symmetric coordinates can be defined easily according to ref 35.

For performing the normal-mode analysis, the DFT harmonic force fields first are transformed from the Cartesian coordinates into the local internal ones. From the GAUSSIAN calculation, the Cartesian force constant matrix F^{c} is obtained. But in the process of normal-mode analysis, the local internal coordinate force constant matrix F^{in} used to be read. The former can be transformed to the latter by the relationship of $F^{\mathrm{in}} = B^{+}F^{\mathrm{c}}B$, where B^{+} is an inverse of a transformation matrix, B.[36,37,38] Then, the scaled quantum mechanical force field (SQMF) procedure is carried out,[37]

$$F_{ij}^{\mathrm{scaled}} = (S_i S_j)^{1/2} F_{ij}^{\mathrm{in}} \qquad (2)$$

where S_i is the scaled factor of the coordinate i, F_{ij}^{in} is the DFT force constant in the local internal coordinates, and F_{ij}^{scaled} is the scaled force constant. In this study, these scaled factors for the coordinates of pyridine moiety are taken from the previous paper.[31] The scaling factors are 0.935 for the C−H stretching motions and 0.963 for the ring stretching, the bending, and the out-of-plane modes, which are used to scale the B3LYP force fields of all the target complexes. For the internal coordinates of the stretches, the bends, and the torsion motions involving the metal atoms, the scaling factors of these force constants are set to 1.00. The final vibrational frequencies and the potential

TABLE 1: Calculated Geometries of Py−M_2 (M = Cu, Ag, and Au)

complexes		HF	MP2	SVWN	BLYP	G96LYP	BPW9 1	G96PW9 1	B3PW9 1	B3LYP[a]
Py−Cu_2	N_1−Cu_{12}	2.185	1.982	1.890	2.005	1.998	1.983	1.976	2.013	2.033
	Cu_{12}–Cu_{13}	2.436	2.344	2.193	2.279	2.271	2.271	2.263	2.281	2.286
	N_1–C_2	1.325	1.349	1.341	1.361	1.359	1.356	1.354	1.341	1.344
	C_2–C_3	1.382	1.395	1.380	1.398	1.396	1.394	1.393	1.387	1.390
	C_2–N_1–C_6	118.4	118.0	118.4	117.8	117.8	117.9	117.8	118.2	118.2
Py−Ag_2	N_1−Ag_{12}	2.531	2.328	2.163	2.384	2.376	2.343	2.333	2.353	2.382
	Ag_{12}–Ag_{13}	2.733	2.674	2.508	2.621	2.608	2.593	2.578	2.595	2.616
	N_1–C_2	1.323	1.347	1.335	1.353	1.352	1.349	1.347	1.337	1.340
	C_2–C_3	1.383	1.396	1.383	1.401	1.399	1.397	1.395	1.389	1.391
	C_2–N_1–C_6	118.2	117.9	118.8	118.1	118.1	118.1	118.1	118.2	118.2
Py−Au_2	N_1–Au_{12}	2.304	2.132	2.041	2.125	2.151	2.125	2.113	2.137	2.167
	Au_{12}–Au_{13}	2.613	2.585	2.489	2.549	2.570	2.549	2.538	2.543	2.567
	N_1–C_2	1.326	1.350	1.340	1.354	1.357	1.354	1.352	1.342	1.345
	C_2–C_3	1.381	1.394	1.380	1.394	1.396	1.394	1.393	1.387	1.389
	C_2−N_1–C_6	118.5	118.4	119.0	118.5	118.5	118.5	118.5	118.6	118.6

[a] From ref 32.

energy distributions (PED) are derived by the Wilson's GF matrix method from the SQMF-DFT force field.[38,39]

The coupling of totally symmetric vibrational modes of interest is analyzed according to the perturbation method.[31,40] To make clear the dependence of the coupling of vibrational modes on the different complexes, we mainly consider the coupling of υ_1 and υ_{6a} modes of pyridine moiety, the N−M stretch, and the M−M stretches. The reason that we select both υ_1 and υ_{6a} modes is mainly due to the strong coupling between the vibrations and the N−M stretch.[31] Finally, we also compare the difference of the coupling in Py−Cu_n, Py−Ag_n, and Py−Au_n.

Results and Discussions

Geometry. The experimental and calculated geometries for pyridine and metal dimers are given in the Supporting Information. By inspection of the calculated results, several observations can be made. First, the optimized geometry obtained by the B3LYP method has the best agreement with the experimental geometry.[4,31] Second, an order of the change of the bond distances was observed. For the C−C and C−N bonds, the order is BLYP, G96LYP, BPW91, G96PW91, B3LYP, B3PW91, and SVWN. For the C−H bond, it is clear that the bond length calculated by SVWN is overestimated, in accordance with the previous observations.[41] Third, the bond distances of metal dimers are overestimated with the exception of the bond lengths for M_2 determined by SVWN. The SVWN method always underestimates the metal−metal bond length by up to 2% and overestimates the binding energy by up to 100%.[42−45] The ab initio methods predict the longer bond distances of three dimers than those with all DFT methods.[43] In summary, the results discussed above show that the geometries of pyridine and M_2 predicted with the nonlocal and hybrid DFT methods are in a good agreement with the experimental data.

The geometries for the Py−M_2 complexes calculated by using various methods are provided in Table 1. The trend of the change of the bond distances in the pyridine moiety has been discussed in detail on the basis of the bonding interaction in the previous papers.[31,32] The stronger the bonding is, the larger the change the bond distance is. The extent of the change of M−M bond distances is different in the Py−M_2 complexes. The results calculated for the three complexes by using the present methods shows that the Cu−Cu bond distance increases clearly, whereas the bond distances of Ag−Ag and Au−Au change very small, even a decrease in the bond distances was predicted. This has also been observed in a Au_2O_2 cluster.[46]

The order of the bond distances of the N−M bonds in three complexes are $R_{N-Ag} > R_{N-Au} > R_{N-Cu}$. We interpret this case according to two factors. The one is that the bonding is stronger in Py−Cu_2 and Py−Au_2 than that in Py−Ag_2, as we will see below. The other one is that the relativistic effect results in the different extent of the contraction in the atomic radii of three metal atoms.[32,43] Clearly, the relativistic effect is the smallest for the copper atom. However, its radius itself is relatively smaller than those of silver and gold. Although the electrons fill up to the 6s orbital for gold atom, the effect leads to the lattice constant (4.08 Å) of gold that is slightly smaller than the radius (4.09 Å) of silver.[43] Thus, both factors cause together the above order of the change of the N−M bonds in the three complexes. The average bond distances in Py−M_2 are probably about 1.98−2.03 Å for the N−Cu bond, 2.11−2.18 Å for the N−Au bond, and 2.33−2.38 Å for the N−Ag bond. The N−Cu bond distance is in a quite good agreement with the experimental value of 2.00 (±002) Å measured by using the photoelectron diffraction method for pyridine adsorbed on Cu(110).[27] For silver and gold, there are no direct experimental data for comparison. For the Py/Ag system, Lombardi et al. suggested the N−Ag bond length should be close to about 2.32 Å.[11d] However, the recent theoretical study reported the shortest N−Au bond length of 2.43 Å for pyridine at the on-top site on Au(111) at the low coverage.[47] The bond distance is obviously larger than all our calculated values, 2.11−2.18 Å by using MP2 and DFT methods. Similar to the Cu−N bond distance, our calculated results provide the values of Ag−N and Au−N bond lengths that are probably close to their experimental values at chemisorption states.

Binding Energy. Table 2 presents the binding energies of Py−M_2. Here, we compare the calculated results with the experimental and theoretical values in the literature as possible.[31,32,48−51] First, the binding energy for Py−Ag_2 calculated by all the methods we used is the smallest among three complexes, indicating the weakest bonding in Py−Ag_2. The zero-point energy correction cannot change the order of the binding energies of Py−M_2 (M = Cu, Ag, and Au). By examination of the results in Table 2, one can see that the nonlocal and hybrid DFT methods predict well the binding energies. For example, they are about 20.2−23.6 kcal/mol for Py−Cu_2, 8.9−11.1 kcal/mol for Py−Ag_2, and 24.5−28.9 kcal/mol for Py−Au_2. The HF (SVWN) method underestimates (overestimates) the binding energies for the three complexes. The MP2 binding energies are slightly larger than those by using the nonlocal and hybrid DFT methods. As shown in Table 2,

TABLE 2: Calculated Binding Energies of Py−M_2 Complexes by Using ab Initio and Density Functional Theoretical Method with the Basis Sets of 6-311+G(d,p) for C, N, and H Atoms and Lanl2DZ for Cu, Ag, and Au Atoms[a]

methods	Py−Cu_2	Py−Ag_2	Py−Au_2
HF	13.37 (12.48)	7.91 (7.30)	12.88 (11.90)
MP2	28.57 (27.13)	17.54 (16.60)	33.54 (32.03)
SVWN	40.03 (39.00)	25.75 (24.86)	50.14 (48.71)
BLYP	23.68 (22.72)	11.46 (10.67)	27.07 (25.84)
BPW91	24.53 (23.60)	11.87 (11.08)	30.14 (28.85)
G96LYP	21.77 (20.78)	9.70 (8.90)	26.77 (25.51)
G96PW91	22.57 (21.63)	10.10 (9.31)	30.00 (28.66)
B3LYP[b]	21.15 (20.17)	11.46 (10.68)	25.73 (24.51)
B3PW91	21.52 (20.55)	11.62 (10.85)	27.86 (26.59)
B3LYP[b]	25.73	12.94	23.97
B3LYP[b]	25.56	15.40	26.31
literature	22.4[c]	11.8[d]	11[e]

[a] The zero-point energy correction binding energies are listed in the parenthesis. [b] From ref 32. [c] Experimental value from ref 52. [d] Experimental value from ref 53. [e] Theoretical value from ref 47.

changing the metallic dimer to trimer and tetramer, we can see that the binding energies increase to about 25.6 kcal/mol for Py−Cu_3 (Cu_4), and 12.9, 15.4 kcal/mol for Py−Ag_3 and Py−Ag_4, as well as 24.0, 26.3 kcal/mol for Py−Au_3 and Py−Au_4, respectively.[32] These results show that the binding energies predicted with the nonlocal and hybrid DFT methods are in accordance with each other though there are some differences.

Second, comparison of the binding energies of Py−M_2 with Py−M indicates that the bonding is stronger in the former than that in the latter. This is mainly due to the accepted orbital of metal dimers matching well the lone-paired electrons of pyridine in the energy and the symmetry.[31,32,48] On the other hand, the metal atom only provides a half-filled s orbital or p_z orbital for the lone-pair electrons of the pyridine ring. There is a strong Pauli repulsion in a α spin space, resulting in the weak bonding.[31] In Py−M^+, besides the electrostatic interaction, the Pauli repulsion decreases significantly, leading together to the strong bonding between pyridine and metal ions.[31a] Mitchell et al. obtained the binding energies for $CuNH_3$ and $AgNH_3$ less than 11 and 9.5 kcal/mol: Cu_2NH_3 and Ag_2NH_3 about 20 ± 1 and 15 ± 1 kcal/mol, respectively, on the basis of photodissociation action spectra.[49] The interaction of pyridine with noble metal dimers should be similar to ammonia, that is, the donation interaction of the lone-pair electrons plays an important role.

Third, the binding energy is larger for Py−Cu_2 and Py−Au_2 than for Py−Ag_2. This can be understood that the different hybridizations of s-d_{z2} on the three metal atoms reduce the extent of the repulsion between the lone-pair electrons on nitrogen and the occupied orbital on the metal atoms.[32,48,49] Since the energy gap between s and d_{z2} is smaller for Cu and Au than Ag, the hybridization effect is strong in Cu and Au, indicating that the strong bonding takes place in Py−Cu_2 and Py−Au_2 (see Figure 2). Meanwhile, one can see that the lone pair orbital also obviously lowers in Py−Au_2.

Finally, we compare the bonding energy with the experimental results. The interaction between pyridine and small silver clusters (Ag_n, $n = 1-3$) has been reported experimentally.[50,51] The vibrational frequencies of the υ_1 and υ_{6a} modes of pyridine blueshift clearly from Py−Ag to Py−Ag_2 and Py−Ag_3, indicating that the binding interaction is stronger in Py−Ag_2 and Py−Ag_3 than that in Py−Ag.[50] On the other hand, the calculated binding energies agree well with the experimental values for pyridine adsorbed on copper and silver surfaces.[52,53] On Cu(110) and Ag(111) surfaces, the binding orientations have been shown that the adsorbed pyridine is preferred to the upstanding or slightly tilted configuration via the N-end.[26,27,52,] Lee et al. estimated the zero-coverage desorption activation energy of pyridine adsorbed on Cu(110) to be 22.4 kcal/mol by fitting the temperature programmed desorption spectra.[52] Our calculated binding energies with the zero-point energy correction are in a good agreement with the above experimental value. Yang et al. estimated the binding energy of pyridine on Ag(111) according to temperature programmed desorption spectra.[53] They obtained the binding energies of the four peaks, both the larger binding energies of which are about 11.5−11.8 kcal/mol.[53] This indicates again that the present methods are reliable in prediction of the chemical interaction between pyridine and metal. However, the binding energy between pyridine and Au clusters in the present work is obviously larger than 11 kcal/mol predicted after considering a contribution of the dispersion energy in the recent theoretical calculation on the system of pyridine adsorbed on Au(111) surface.[47] In addition, pyridine is known to adsorb more strongly to gold than to silver.[54] Owing to the similarity in the bonding mechanism of pyridine with Cu and Au, our result calculated by the present methods should be reliable to the binding energy of pyridine/gold in the chemisorption state.

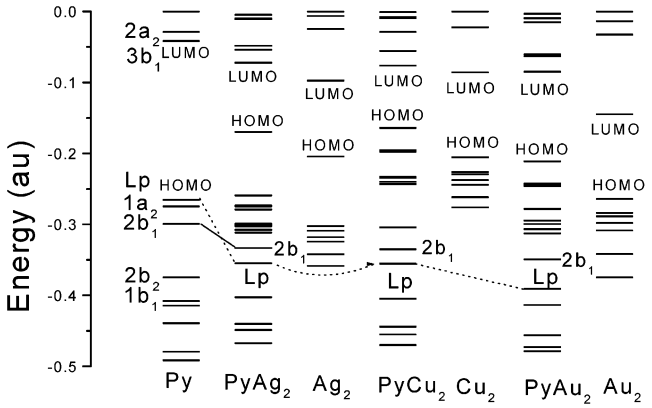

Figure 2. Energy levels of pyridine, Py−Ag_2, Ag_2, Py−Cu_2, Cu_2, Py−Au_2, and Au_2 complexes. The energies (in au.) of the orbitals are calculated at the B3LYP/6-311+G(d,p) (C, N, H)/LanL2DZ(M) level.

Vibrational Frequency. The calculated vibrational frequencies of free pyridine and Py−M_2 are presented in Table 3. Since three A_2 modes are not only infrared inactive, but also their intensities are very weak in the Raman spectrum, their frequencies are not listed here. As shown in Table 3, the SQMF procedure can reproduce well the experimental frequencies of the isolated pyridine molecule in Ar matrix-isolated IR and Raman spectra.[5,31] The larger deviations are only found in the υ_3 mode with a B_2 symmetry, for example, the experimental frequency of 1227 cm^{-1} and the theoretical frequencies of 1259.7 cm^{-1}. The vibrational frequency of the mode is very dependent on the theoretical method.[31,36,55−60] In the previous paper,[31a] on the basis of the observed Raman spectra we suggested the fundamental of the υ_3 mode should be 1260 cm^{-1} instead of the assigned value of 1227 cm^{-1}.

For Py−M_2 complexes, we discuss the shift of vibrational frequencies of the modes of interest. These spectral bands with strong IR and Raman intensities are discussed here, for example, the bands of υ_1, υ_{12}, υ_{6a}, υ_{8a}, and υ_{9a} modes in the A_1 species in the Raman spectra and the bands of υ_4 (B_1), υ_{11} (B_1), and υ_{19b} (B_2) in infrared spectra.

First, the vibrational frequencies of totally symmetric modes υ_1, υ_{12}, υ_{6a}, and υ_{8a} all blueshift because of the interaction between pyridine and metal dimers with respect to the fundamentals of vibrational modes of the free pyridine molecule. The

TABLE 3: Calculated Infrared Intensities (km/mol) of Vibrational Modes Compared with Experimental Infrared Intensities of Free Pyridine and Py−M_2 Complexes

	Py							Py−Cu_2		Py−Ag_2		Py−Au_2	
modes	freq	expt[a]	I_{IR}[b]	I_{IR}[c]	I_{IR}[d]	I_{IR}[e]	I_{IR}[f]	freq	I_{IR}	freq	I_{IR}	freq	I_{IR}
υ_2	3088. 7	0.0	9.3	10.7	8.9	7.2	6.1	3099. 2	11.2	3097.2	13.6	3105.6	11.5
υ_{13}	3065. 4	1.5	3.7	4.0	3.7	4.9	4.6	3080. 8	0.0	3076.5	0.0	3093.3	0.0
υ_{20a}	3046. 0	8.5	6.1	5.7	5.3	4.1	3.9	3071. 8	6.5	3067.2	4.2	3077.0	1.7
υ_{8a}	1592. 4	17.9	20.4	20.1	20.6	23.9	24.3	1607. 9	13.9	1605.4	38.5	1610.8	18.9
υ_{19a}	1482. 0	4.0	2.0	1.7	2.2	2.5	2.8	1484. 8	2.7	1485.4	0.0	1484.3	0.5
υ_{9a}	1218. 0	4.3	4.2	4.3	4.2	4.7	4.7	1214. 0	12.6	1217.2	34.4	1215.3	16.7
υ_{18a}	1072. 4	4.5	6.0	4.5	1.3	5.2	6.6	1069. 9	16.1	1071.7	27.5	1071.2	22.2
υ_{12}	1027. 0	7.7	4.2	6.7	6.3	6.3	4.0	1036. 0	9.5	1030.8	9.2	1037.1	4.5
υ_1	991.3	5.4	5.2	4.2	4.1	4.8	5.8	1009. 5	5.2	1005.6	23.3	1012.2	8.9
υ_{6a}	605.1	4.4	3.2	3.3	3.2	3.6	3.5	635.1	4.9	623.9	15.9	635.7	6.3
υ_5	994.8	0.0	0.0	0.0	0.0	0.0	0.0	997.2	0.1	1000.1	0.1	1007.7	0.1
υ_{10b}	939.4	0.0	0.0	0.0	0.2	0.0	0.0	943.1	0.0	943.1	0.0	952.9	0.2
υ_4	745.2	12.9	8.4	9.8	9.3	11.8	11.6	748.1	29.8	747.9	25.8	758.7	27.7
υ_{11}	702.8	67.5	69.0	66.4	68.6	68.7	70.2	695.5	46.6	698.8	49.7	698.6	52.5
υ_{16b}	410.8	7.2	3.6	3.8	3.6	4.0	3.8	421.8	1.5	419.2	1.7	432.7	1.5
υ_{20b}	3081. 1	15.9	28.7	32.5	27.4	25.5	22.3	3093. 7	10.2	3091.3	11.7	3101.9	4.1
υ_{7b}	3043. 7	5.1	31.4	31.3	31.1	28.0	27.9	3075. 5	1.4	3068.0	4.7	3089.0	0.8
υ_{8b}	1586. 9	7.3	8.6	7.3	8.6	10.1	11.1	1582. 0	1.3	1586.6	2.5	1583.3	1.1
υ_{19b}	1442. 0	31.1	24.1	24.4	24.6	27.0	27.3	1447. 7	29.7	1447.8	30.3	1450.9	29.6
υ_{14}	1357. 9	0.5	0.0	0.0	0.0	0.1	0.0	1357. 4	2.5	1358.9	2.0	1357.3	1.8
υ_3	1259. 7	0.0	0.3	0.4	0.2	0.0	0.0	1263. 9	0.4	1264.8	0.5	1263.1	1.7
υ_{15}	1148. 3	3.6	1.8	1.9	1.7	2.4	2.3	1154. 7	2.3	1153.9	2.6	1256.5	2.5
υ_{18b}	1056. 0	0.0	0.0	0.0	0.0	0.0	0.0	1066. 6	1.9	1065.4	1.3	1070.4	1.9
υ_{6b}	656.8	1.1	0.3	0.3	0.4	0.3	0.4	652.5	0.0	653.6	0.0	651.6	0.0
RASD[g]			6.7	7.0	6.5	5.7	5.6						

[a] From ref 36. [b] BPW91. [c] G96LYP. [d] G96PW91. [e] B3LYP. [f] B3PW91. [g] The root-average-squared deviation RASD = $\sqrt{\sum_{i=1}^{24}(IR^i_{The} - IR^i_{Exp})^2/24}$.

extent of the frequency shift depends on the strength of the bonding in Py−M_2.[16,30,31,61] From Table 3, we can see that the frequency of the υ_1 mode increases from 991.3 cm^{-1} in free pyridine to 1009.5, 1005.6, and 1012.2 cm^{-1} in Py−Cu_2, Py−Ag_2, and Py−Au_2; for the υ_{6a} mode from 605.1 cm^{-1} to 635.1, 623.9, and 635.7 cm^{-1} in Py−Cu_2, Py−Ag_2, and Py−Au_2, respectively. Owing to the strong bonding in Py−M_2, these vibrational frequencies obviously have larger blueshifts than those calculated in Py−Cu, Py−Ag, and Py−Au.[31] In fact, this is also supported by the infrared spectra observed by Tevault and Smardzewski on the system of pyridine interacting with small silver clusters in the argon matrix reactions.[50] They observed two bands at 614 and 1000 cm^{-1} with a relatively low concentration of silvers. With increasing Ag atom concentration, they found two new bands at 626 and 1010 cm^{-1}. On the basis of the experimental result, they assigned the former species to Py−Ag while for the latter set they assigned to the most likely reaction product, Py−Ag_2. The previous SQMF−B3LYP calculation has predicted that the fundamentals of υ_{6a} and υ_1 modes are about 615.9 and 999.0 cm^{-1} for Py−Ag.[31] This indicates that our calculated frequencies are in a quite good agreement with the experimental frequencies. For comparison, Tevault and Smardzewski also reported vibrational frequency shifts of these two modes because of the interaction between pyridine and a Cu atom. For example, the experimental values of both two modes of Py−Cu are 624 and 1007 ± 2 cm^{-1}, well compared with the SQMF−B3LYP vibrational frequencies of 625.4 and 1004.2 cm^{-1}.[31] Krasser et al. reported Raman spectra of silver−pyridine clusters. [51] However, owing to forming the amorphous carbon in the experimental process, it possibly influences the quality of Raman spectra. In the range of 1000−1050 cm^{-1} they observed two sharp bands, 994 and 1038 cm^{-1}, which are the strongest in the vibrational Raman spectra of free pyridine. For Py−Ag_4^+, Vivon et al. predicted the vibrational frequencies of υ_{6a} and υ_1 modes to be 629 and 1003 cm^{-1} at the HF/Land2DZ level.[11d]

Second, the vibrational frequency shifts of the υ_4 (B_1) and υ_{11} (B_1) modes are not only opposite but also small. The frequency of the υ_4 mode increases from 745 cm^{-1} to 748−759 cm^{-1}, while the frequency of the υ_{11} mode decreases from 703 cm^{-1} to 696−699 cm^{-1} because of the interaction between pyridine and metal dimers. Tevault and Smardzewski observed a band at 693 cm^{-1}, very close to the calculated frequency of 695.2 cm^{-1} in Py−Cu.[31,50] Since they focused on the vibrational modes with the Raman enhancement effect, there is no experimental value for a systematical comparison of the two strong infrared active modes.

Third, among the B_2 modes, the vibrational frequency of the υ_{19b} mode shifts slightly with respect to the value of 1442.3 cm^{-1} of free pyridine. The experimental frequency of the vibrational mode is 1445.9 cm^{-1} observed by infrared spectroscopy for pyridine−silver reaction product.[50] The calculated frequencies are 1446.2 and 1447.8 cm^{-1} for Py−Ag[31] and Py−Ag_2, 1447.4 and 1447.7 cm^{-1} for Py−Cu[31] and Py−Cu_2, and 1448.2 and 1450.9 cm^{-1} for Py−Au[31] and Py−Au_2, respectively. The band corresponding to the vibrational frequency is easy to be observed in infrared spectra of pyridine adsorbed on metal surfaces.[21−25] Finally, the vibrational frequencies of all C−H stretching modes blueshift because of the interaction between pyridine and metal dimers. The order of the extent of the blueshift is Py−Au_2 > Py−Cu_2 > Py−Ag_2.

Infrared Intensity. As a model system of pyridine adsorbed on metal surfaces, numerous experimental infrared spectra have been reported.[21−25] However, there is no systemically theoretical calculation for checking the validity of the theoretical method in predicting the infrared intensities of vibrational modes of the free pyridine molecule and pyridine interacting with the metals. Here, our calculated results are presented in Table 3 for free pyridine and Py−M_2 complexes, respectively. First, we compare

TABLE 4: Calculated Frequencies (cm^{-1}) of the Low-Frequency Totally Symmetric Vibrational Modes of $Py-M_2$

mode	HF	MP2	SVWN	BLYP	BPW91	G96LYP	G96PW91	B3LYP	B3PW91
υ_{N-Cu}	120.5	156.9	192.8	162.2	165.6	163.4	166.2	154.4	157.7
υ_{Cu-Cu}	216.9	279.1	338.8	286.9	292.3	289.2	294.0	276.5	280.7
υ_{N-Ag}	84.2	111.9	142.2	106.2	108.6	106.3	107.6	106.9	108.9
υ_{Ag-Ag}	157.0	192.3	238.0	190.8	198.5	193.2	201.3	192.1	197.8
υ_{Au-Au}	113.7	146.5	167.7	133.7	144.5	137.1	148.6	136.9	145.0
υ_{N-Au}	172.2	214.5	249.7	196.6	213.4	201.9	217.9	199.3	211.4

the results calculated for free pyridine with experimental spectral intensities (see Table 3).[36] One can see that for pyridine in the gas phase the strongest band in the experimental infrared spectrum arises from the υ_{11} mode that has an intensity of 67.5 km/mol. The value can be predicted well by use of HF, BLYP, BPW91, G96LYP, G96PW91, B3LYP, and B3PW91 methods. However, the MP2 method predicts the IR intensity of the vibration only to be 6.1 km/mol. Conversely, the intensity of the υ_4 mode calculated by the MP2 method is 77.7 km/mol. This is clearly different from the results of the other theories in this work and the IR experiment.[23,36] Also, the HF and BLYP methods overestimate the intensities of the υ_{8a} mode (experiment: 17.9 km/mol; theory: 42.5 km/mol) and the υ_{12} mode (experiment: 7.7 km/mol; theory: 32.5 km/mol), respectively. Both nonlocal DFT methods (such as BPW91, G96LYP, and G96PW91) and hybrid DFT methods (B3LYP and B3PW91) can provide a good prediction on the infrared intensities of various vibrational modes of free pyridine. Further, the deviations of theoretical IR intensities with respect to the experimental values are shown in the last row in Table 3. The small deviations imply that the intensities of the hybrid DFT methods are the best agreement with the experimental ones.[36] This is a reason we only show the IR intensities of $Py-M_2$ complexes calculated by the hybrid DFT method (B3LYP) in Table 3.

The change of IR intensities of the vibrations in $Py-M_2$ depends on the property of the vibrational mode. From Table 3, we can see that the interaction between pyridine and Ag_2 enhances the infrared intensities of vibrational modes in the A_1 species. If the enhancement factor is defined as a ratio of the intensity of the given vibrational mode in $Py-Ag_2$ and the intensity of the corresponding mode in the free pyridine molecule, we can obtain the enhancement factors about 7.3 (υ_{9a}), 5.6 (υ_{18a}), 5.1 (υ_1), 4.3 (υ_{6a}), and 1.6 (υ_{8a}) predicted by B3PW91 and about 7.3 (υ_{9a}), 4.2 (υ_{18a}), 4.0 (υ_1), 4.6 (υ_{6a}), and 1.6 (υ_{8a}) predicted by B3LYP. The IR intensity of the υ_{8a} mode is still the strongest among these enhanced modes though the mode has a small enhancement factor. For both B_1 modes of interest, the enhancement of two folds is found in the υ_4 mode, while the decrease of the IR intensity is done in the υ_{11} mode. The latter mode still has the largest value of IR intensity of 49.7 and 52.1 km/mol predicted by B3LYP and B3PW91, respectively. Among B_2 modes the IR intensities of the υ_{19b} mode predicted by B3PW91 and B3LYP are 31.4 and 30.3 km/mol, respectively. Both values are slightly larger than the values calculated for the free pyridine.

The IR intensity of the vibrational mode depends on the metal property. As mentioned above, the bonding is stronger in $Py-Cu_2$ and $Py-Au_2$ than that in $Py-Ag_2$. This results in that the vibrational modes of υ_1, υ_{6a}, υ_{9a}, and υ_{18a} have smaller IR intensities in $Py-Cu_2$ and $Py-Au_2$ than those in $Py-Ag_2$. On the other hand, the change of the IR intensities is small for the υ_4 and υ_{11} modes in the B_1 species and the υ_{19b} mode in the B_2 species. There, it was interpreted that the strong bonding interaction changes the properties of the vibrational modes, resulting in the decrease of the derivatives of the dipole moment and the polarizability with respect to the normal coordinate of the given mode.[31,62]

The IR spectra of pyridine adsorbed on metal surfaces have been observed. Owing to the IR surface selection rule, one used to observe vibrations with the transition dipole moment perpendicular to the surface.[21,23] For pyridine adsorbed on the Cu(110) surface, the pyridine molecule is bound to the Cu(110) surface through the N-end upright orientation in the first layer. The in-plane vibrations, for example, υ_1, υ_{12}, υ_{8a}, υ_{18a}, and υ_{19b} modes, can be observed.[21] On the other hand, the band from the υ_{11} mode, which is very strong in the gas phase, cannot be observed because of the transition dipole moment parallel to the Cu surface. For pyridine adsorbed on a polycrystalline Au electrode, the out-of-plane bending mode υ_4 was observed at negative potentials at the low bulk concentration. As positively moving potential, the intensities of the vibrations of υ_{19b} and υ_{8a} increase significantly because of the change from the flat to the upright orientation. At the same time, the vibrations of υ_1, υ_{12}, υ_{18a}, and υ_{9a} appear because of the reorientation of pyridine.[23]

Vibrational Couplings. Numerous studies have discussed the vibrational frequency shift of the internal modes of pyridine because of the interaction with hydrogen-bond molecules,[7,63] metal ions,[61,64] oxides,[65] and metal surfaces.[11,12,16,17,30] Recently, the frequency shift of the vibrational modes in the A_1 species was explored theoretically on the basis of the interaction of pyridine and single metal atoms and ions.[31] Here, we discuss our calculated results for the system of pyridine interacting with small metal clusters. First, we present vibrational frequencies of the N−M stretch and the M−M one in $Py-M_2$ in Table 4. Comparing the vibrational frequencies with the binding energies predicted by HF and SVWN methods, we believe that the HF method underestimates the two vibrational frequencies while the SVWN method does conversely. Since the vibrational frequencies of both modes are in a good agreement with each other from MP2, nonlocal DFT, and hybrid DFT, we will discuss the results calculated by using the B3LYP method below.

On the basis of normal-mode analysis, we have provided an assignment of the vibrational frequencies to the M−M and N−M stretches. For example, in $Py-Cu_2$, the higher frequency at the range of 276.5−294.0 cm^{-1} is assigned to the Cu−Cu stretch; the lower frequency at the range of 154−166.2 cm^{-1} is done to the N−Cu stretch. For $Py-Ag_2$ the assignment is the same as that in $Py-Cu_2$. This also agrees well with the PED values for two vibrations. We obtained that the PED values are 78 (Ag−Ag) and 20 (N−Ag) for 192.1 cm^{-1}, 73 (N−Ag) and 22 (Ag−Ag) for 106.8 cm^{-1}, 68 (Cu−Cu) and 29 (N−Cu) for 276.3 cm^{-1}, and 56 (N−Cu) and 32 (Cu−Cu) for 154.2 cm^{-1}. But for $Py-Au_2$, there exists a large mixing between the N−Au stretch and the Au−Au one. The normal-mode analysis indicates that the PED values are 46 (N−Au) and 39 (Au−Au) for 199.1 cm^{-1} and 47 (N−Au) and 53 (Au−Au) for 136.7 cm^{-1}. Thus, we provide a tentative assignment that the N−Au stretch has the vibrational frequency to be 199.1 cm^{-1}, whereas the frequency of the Au−Au stretch is 136.7 cm^{-1}. The assignment

TABLE 5: Calculated Frequencies (cm^{-1}) and Stretching Force Constants (mdyn/Å) of the N−M and M−M Stretching Vibrations with the Totally Symmetric Property in Py−M_n (M = Cu, Ag, Au; n = 1−4) Complexes at the B3LYP/6-311+G(d,p) (C, N, H)/LANL2DZ Level

complex	ω_1	ω_2	ω_3	f_{N-M}	f_{M-M}	f_{M-M}
Py−Cu	162.0 (261.1)[a]		244[b]	0.58 (1.73)[a]		
Py−Ag	86.4 (184.6)[a]		235[b]	0.21 (1.02)[a]		
Py−Au	106.8 (225.5)[a]		260[b]	0.40 (2.09)[a]		
Py−Cu_2	276.5	154.4	256.2 (265)[c]	0.97	1.11	1.22 (1.30)[c]
Py−Ag_2	192.1	106.9	177.1 (192.4)[c]	0.49	0.99	0.99 (1.17)[c]
Py−Au_2	199.3	136.8	162.3 (190.9)[c]	1.12	1.66	1.53 (2.11)[c]
Py−Cu_3	273.5	164.4	115.3	1.16	0.79	0.91/0.66[d]
Py−Ag_3	182.3	109.1	69.3	0.58	0.63	0.56 (0.59)[d]
Py−Au_3	188.9	128.0	80.7	1.18	0.91	1.25[d]
Py−Cu_4[e]	274.3 (277.1)	179.3 (180.8)	132.4 (133.6)	1.13 (1.16)	0.43 (0.44)	0.67 (0.68)
Py−Ag_4[e]	184.4 (188.2)	124.5 (123.0)	93.9 (94.0)	0.61 (0.58)	0.37 (0.36)	0.52 (0.53)
Py−Au_4[e]	194.2 (194.1)	136.2 (136.2)	87.1 (87.1)	1.23 (1.23)	0.36 (0.36)	0.88 (0.90)

[a] From ref 31. The values in the parenthesis correspond to the vibrational frequencies and the force constants in the cation Py−M complexes. [b] From experimental Raman spectra: 244 cm^{-1} from ref 14 and 10a; 235 cm^{-1} from ref 11a; 260 cm^{-1} from ref 10a. [c] The values in the parenthesis from ref 42 correspond to the vibrational frequencies and the force constants of the isolated metal dimers. [d] The force constants of the isolated trimers are from ref 42. [e] The values in the parenthesis are the vibrational frequencies of the low-frequency totally symmetric modes in Py−M_4 with the perpendicular orientations between pyridine ring and M_4 ring.

is clearly different from the experimental frequency of 190.9 cm^{-1} for free Au_2.[42,43]

Under the harmonic approximation, vibrational frequencies and force constants of the N−M and M−M stretches are presented in Table 5. They are calculated by use of the B3LYP method. We can summarize these results as following. (1) All the theoretical vibrational frequencies in Py−Ag, Py−Ag_2, and Py−Ag_3 are less than the value of 235 cm^{-1}. The latter one was observed in the Raman spectra of pyridine interacting with small silver cluster[51] and with the N-end adsorption on silver surfaces. Our calculated results indicate that the N−Ag stretch should have a low vibrational frequency, for example, 86.4 cm^{-1} in Py−Ag, 106.9 cm^{-1} in Py−Ag_2, and 109.1 cm^{-1} in Py−Ag_3. The symmetric Ag−Ag stretching frequencies are 192.1 and 182.2 cm^{-1} for Py−Ag_2 and Py−Ag_3, respectively. In Py−Ag_3, the Ag−Ag−Ag bending-mode frequency that cannot be observed so far is predicted to be 69.3 cm^{-1}. The experimental Raman spectrum of the mixture of small Ag clusters shows that there are only two sharp bands at about 190 and 120 cm^{-1}, which can be assigned to the Ag−Ag stretching vibration and the symmetric stretching one in Ag_2 and Ag_3, respectively.[32,42,51] For Ag_3, the asymmetric stretching frequency is observed at 161.1 and 157.9 cm^{-1}, which can be predicted well at 159.1 cm^{-1} by B3LYP for the electronic ground states of the isolated Ag_3 with the obtuse geometry though it was not observed in the Raman experiment.[32,66,67] On the other hand, there are three bands (120, 190, and 235 cm^{-1}) observed in the low-frequency Raman spectrum of Py−Ag_n (n = 1−3), where the band at 120 cm^{-1} is very sharp while the band at 190 cm^{-1} is very broad.[51] Comparison of these theoretical and experimental data indicates that it is reliable to propose an assignment that the N−Ag stretching vibration gives rise to the band at about 120 cm^{-1}, while the Ag−Ag stretches in Py−Ag_2 and Py−Ag_3 yield the broad band at about 190 cm^{-1}. For the experimental band observed at 235 cm^{-1}, we propose that it is probably an overtone of the N−Ag stretching vibration in the Raman experiment.[51] In Py−Ag_4, the vibrational frequencies are also all less than 200 cm^{-1}. The frequency of 124.4 cm^{-1} may be assigned to the N−Ag stretch. The theoretical binding energy is in agreement with the experimental values (see Table 2), indicating that the present methods are reliable in describing the chemical bonding between pyridine and silver. The force constants of the N−Ag stretches in these complexes are in the range of 0.49−0.61 mdyn/Å smaller than the values of 1.0, 1.1, and 1.5 mdyn/Å.[11a,11d,29] These force constants were assumed by fitting to the low-frequency band at about 235 cm^{-1} in Raman spectra. (2) The mass effect results in that the direction of the vibrational frequency shift is opposite in Py−M_n cluster complexes. Although the force constant of the Au−Au bond is larger than the force constant of the N−Au bond in Py−Au_2 (see Table 5), the unperturbed frequencies are 183.7 and 169.2 cm^{-1} for υ_{N-Au} and υ_{Au-Au} stretches in Py−Au_2, respectively, on the basis of the harmonic approximation. Because of the small difference (12.5 cm^{-1}) of both unperturbed frequencies, they should have a strong vibrational coupling. In terms of the Herzberger's ideal, the coupling results in that the higher frequency is shifted up and the lower frequency is shifted down.[40] If we neglect the coupling between the Au−Au stretching mode and the other A_1 modes of the pyridine moiety, we can obtain the perturbed frequencies of about 216.6 and 136.8 cm^{-1} because of the coupling shifts of the unperturbed frequencies when the perturbation term is close to 39.5 cm^{-1} (see Figure 3A). The large frequency of the N−Au stretch will decrease because of the coupling between the N−M stretch and the υ_{6a} and υ_1 modes. In Figure 3B, we can obtain that the frequency shift of Py−Ag_2 is opposite to that in Py−Au_2. For Py−Au_3 and Py−Au_4, the frequencies of 188.9 and 194.2 cm^{-1} are assigned to the N−Au stretching modes. However, the two modes contain considerable amount of metal motions, as Moskovits discussed the N−Ag stretch in Py−Ag_4.[29] For example, the PED values are 65 N−Au and 35 Au−Au for 188.9 cm^{-1}, 73 Au−Au and 21 N−Au for 128.0 cm^{-1} in Py−Au_3; 62 N−Au and 15 metal ring vibration for 193.9 cm^{-1}, 43 metal ring vibration and 21 N−Au for 136.1 cm^{-1} in Py−Au_4. (3) The coupling between the N−Cu stretch and the symmetric ring bend is strong in Py−Cu_4. We can see that the force constants of the M−M bonds close to the N−M bond decrease significantly from Py−Cu_2 to Py−Cu_4. This causes a decrease of the coupling between the N−M stretch and the M−M symmetric one. For Py−Cu_4, the PED values of the mode with the vibrational frequency of 274.3 cm^{-1} are 36 N−Cu, 22.3 Cu_4 ring-bending coordinate, and 17 Cu−Cu.

Second, among the A_1 modes, the vibrational frequency shifts of the υ_1 and υ_{6a} modes depend on the strength of the bonding between pyridine and metal clusters. In Figure 4, we show the variations of the vibrational frequency on the size of the metal clusters and the force constants of N−M bonds. The binding energies of these complexes indicate that the strong chemical bonding takes place in the Py−M_2, Py−M_3, and Py−M_4. The weak bonding only was formed in Py−M. In Figure 4A, the

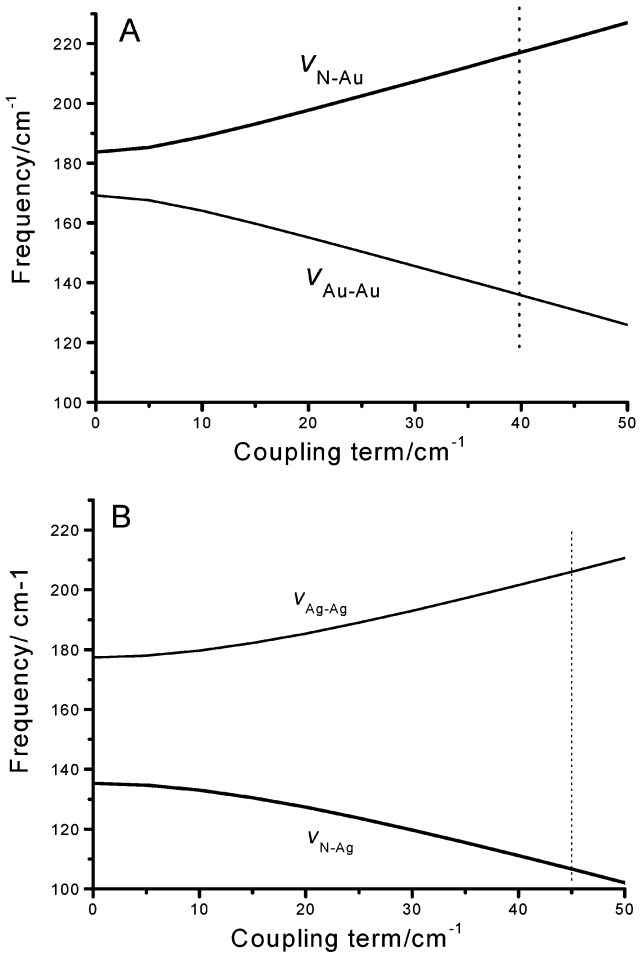

Figure 3. Vibrational couplings between the N−M stretch and the M−M stretch in (A) Py−Au_2 and (B) Py−Ag_2.

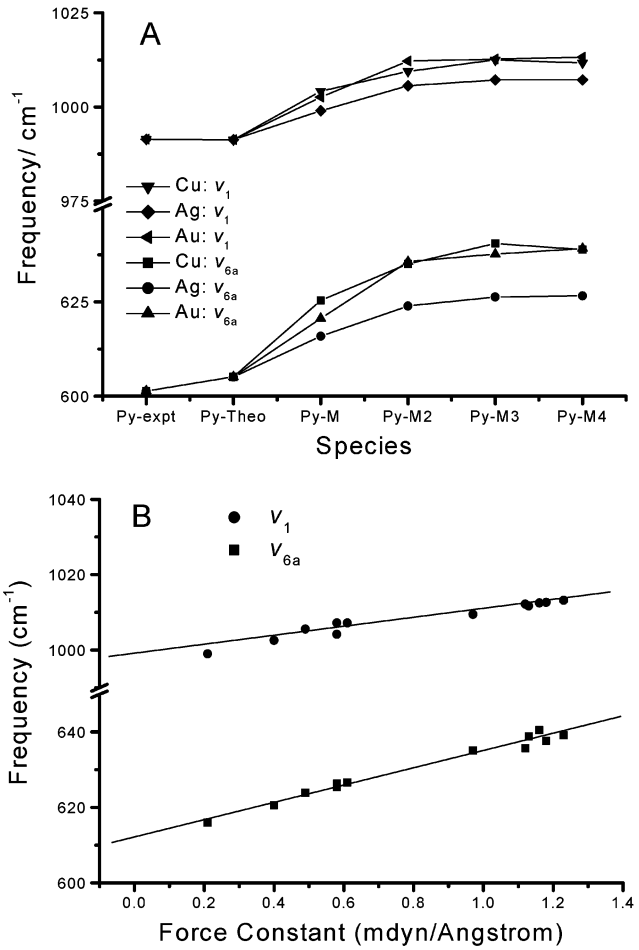

Figure 4. Changes of vibrational frequencies of the υ_1 and υ_{6a} modes among Py−M_n (M = Cu, Ag, and Au; n = 0−4) with (A) the size of metal clusters and (B) the force constants of the N−M stretching vibration.

vibrational frequency increases with the size of the metal clusters. However, the trend of the increase of vibrational frequency becomes flat at Py−M_3 and Py−M_4. This is mainly because the force constants of the N−M stretches have a small change for both complexes because of almost the same strength of the bonding (see Table 5). Figure 4B shows the change of the vibrational frequencies of the υ_1 and υ_{6a} modes with the force constants of the N−M stretches. We can see the good linear relationships of the υ_1 and υ_{6a} frequencies on the N−M force constant. The best fitting linear relationships to the calculated vibrational frequencies of Py−M_n (n = 1−4) are υ_1 = 12.42 f_{N-M} + 998.14 with a regression coefficient of 0.97 and υ_{6a} = 22.78 f_{N-M} + 612.15 with a regression coefficient of 0.99. The υ_{6a} mode has about two folds of the slope of the υ_1 mode, indicating that the former vibrational frequency blueshifts more sensitive to the strength of the N−M bond than the latter one. This is in agreement with the previous study that proposed the υ_{6a} mode is a good indicator for a measure of the strength of the pyridine−metal bond.[31] There, the coupling is stronger between the υ_{6a} mode and the N−M stretch than that between the υ_1 mode and the N−M stretch.

Concluding Remarks

The structural and bonding properties of pyridine−metal cluster complexes have been investigated by use of different quantum chemical methods. Our calculated results clearly indicate that the hybrid DFT method can predict well the structural properties, the binding energies, the vibrational frequencies, and the IR spectral intensities of free pyridine and Py−M_n complexes. The change of the structures of the pyridine ring is closely associated with the bonding mechanism, that is, the lone-pair donation interaction and the bonding in the π space. The strength of the bonding depends on the metal property and the binding orientation. On the basis of binding energies calculated by using the different quantum chemical methods, we predict that the binding energy of pyridine chemically adsorbed on gold surface should be a value in the range of 24.0−28.7 kcal/mol via a N-end adsorption.

The vibrational frequency shift of the pyridine ring modes has been discussed in detail in the present paper. Comparison of the calculated and experimental vibrational frequencies indicates that the SQMF−B3LYP procedure can predict well the fundamentals of the pyridine moiety. The results are in a good agreement with the experimental IR spectral peaks for Py−Ag, Py−Ag_2, and Py−Cu. In particular, there are the good linear relationships of the vibrational frequencies of the υ_1 and υ_{6a} modes on the force constants of the N−M bonds. Among all the A_1 modes, the blueshift of the vibrational frequency of the υ_{6a} mode is the most sensitive to the strength of the bonding of pyridine with metal clusters. This is in agreement with the previous study that proposed the vibrational frequency shift of the υ_{6a} mode as an indicator for a measure of the strength of the N−M bond for pyridine adsorbed on metal surfaces. The present study extends the previous conclusion obtained from

the Py−M complex to a system of pyridine interacting with a metal cluster.

One of the main goals in the present paper is to explore the vibrational frequency of the pyridine−metal bond. On the basis of our calculated vibrational frequencies on the pyridine and small clusters, we have provided a new assignment of the experimental Raman spectral bands for $Py-Ag_n$ ($n = 1-3$) cluster complexes. The observed band at 122 cm^{-1} is attributable to the N−Ag stretching vibrations in $Py-Ag_2$ and $Py-Ag_3$. The band observed at 235 cm^{-1} is assigned to the overtone of the N−Ag stretch. On the other hand, the very broad band at about 190 cm^{-1} observed in the Raman spectrum is assigned to the (symmetric) Ag−Ag stretching vibration in $Py-Ag_2$ and $Py-Ag_3$. The reliability of the assignment is supported by three facts. First, the binding energy is comparable to the experimental value for pyridine adsorbed on silver. This indicates that the present theoretical methods are reliable to describe the bonding interaction between pyridine and silver clusters. Second, the blueshifts of the experimental vibrational frequencies are predicted quite well. The vibrational frequency shift is closely associated with the strength of the pyridine−metal bond. We have obtained the linear relationships of the vibrational frequencies of ν_1 and ν_{6a} on the force constants of the N−M stretches. It is in agreement with the previous studies. Third, the force constant of the N−Ag stretch is predicted to be 0.49−0.61 mdyn/Å when the bonding between pyridine and the neutral silver cluster is very strong. Finally, we discuss the coupling between the internal modes and N−M stretch as well as the coupling between the N−M stretch and totally symmetric vibrational modes of the backbone of metal clusters. It is helpful for us to understand the nature of the vibrational frequency shift.

Acknowledgment. We wish to thank the National Science Council (NSC) of ROC, Academia Sinica and the CTCI Foundation for the financial support of this work. One of the authors (M.H.) would like to thank the NSC for financial support (NSC-91-2113-M-002-034).

Supporting Information Available: Table of experimental and calculated geometries of the free pyridine molecule and isolated dimers. This material is available free of charge via the Internet at http://pubs.acs.org.

References and Notes

(1) (a) Yates, J. T., Jr.; Madey, T. E. *Vibrational Spectroscopy of Molecules on Surfaces*; Plenum: New York, 1987. (b) Desjonqueres, M.-C.; Spanjaard, D. *Concepts in Surface Physics*, Second Edition; Springer: Berlin, 1996. (c) Niu, S. Q.; Hall, M. B. *Chem. Rev.* **2000**, *100*, 353.

(2) (a) Chan, J.; Reed, M. A.; Rawlett, A. M.; Tour, J. M. *Science* **1999**, *286*, 1550. (b) Damle, P. S.; Ghosh, Datta, S. *Phys. Rev. B* **2001**, *64*, 201403. (c) Park, J.; Pasupathy, A. N.; Goldsmith, J. I.; Chang, C.; Yaish, Y.; Petta, J. R.; Rinkoski, M.; Sethna, J. P.; Abruna, H. D.; McEuen, P. L.; Ralph, D. C. *Science* **2002**, *417*, 722.

(3) Walters, V. A.; Snavely, D. L.; Colson, S. D.; Wiberg, K. B.; Wong, K. N. *J. Phys. Chem.* **1986**, *90*, 592.

(4) Innes, K. K.; Ross, I. G.; Moomaw, W. R. *J. Mol. Spectrosc.* **1988**, *132*, 492.

(5) Klots, T. D. *Spectrochim. Acta A* **1998**, *54*, 1481, and references therein.

(6) Skinner, J. G.; Nilsen, W. G. *J. Opt. Soc. Am.* **1968**, *58*, 113.

(7) Schlucker, S.; Sighn, R. K.; Asthana, B. P.; Popp, J.; Kiefer, W. *J. Phys. Chem. A* **2001**, *105*, 9983.

(8) Fleischmann, M.; Hendra, P. J.; McQuillan, A. J. *Chem. Phys. Lett.* **1974**, *26*, 163.

(9) (a) Jeanmaire, D. J.; Van Duyne, R. P. *J. Electroanal. Chem.* **1977**, *84*, 1. (b) Dick, L. A.; McFarland, A. D.; Haynes, C. L.; van Duyne, R. P. *J. Phys. Chem. B* **2002**, *106*, 853.

(10) (a) Creighton, J. A.; Blatchford, C. G.; Albrecht, M. G. *J. Chem. Soc., Faraday Trans. 2* **1979**, *75*, 790. (b) Creighton, J. A. *Surf. Sci.* **1986**, *173*, 665. (c) Creighton, J. A. *Progress in Surface Raman Spectroscopy*; Tian, Z. Q., Ren, B., Eds.; Xiamen University Press: Xiamen, 2000; p 11.

(11) (a) Lombardi, J. R.; Knight, E. A. S.; Birke, R. L. *Chem. Phys. Lett.* **1981**, *79*, 214. (b) Sanchez, L. A.; Lombardi, J. R.; Birke, R. L. *Chem. Phys. Lett.* **1981**, *79*, 219. (c) Lombardi, J. R.; Birke, R. L.; Sanchez, L. A.; Bernard, I.; Sun, S. C. *Chem. Phys. Lett.* **1984**, *104*, 240. (d) Vivoni, A.; Birke, R. L.; Foucault, R.; Lombardi, J. R. *J. Phys. Chem. B* **2003**, *107*, 5547.

(12) (a) Pockrand, I.; Otto, A. *Solid State Commun.* **1980**, *35*, 861. (b) Otto, A.; Mrozek, I.; Grabhorn, H.; Akemann, W. *J. Phys.: Condens. Matter* **1992**, *4*, 1143. (c) Bruckbauer, A.; Otto, A. *J. Raman Spectrosc.* **1998**, *29*, 665.

(13) Welzel, H. A.; Gerischer, H.; Pettinger, B. *Chem. Phys. Lett.* **1981**, *80*, 392.

(14) Loo, B. H. *J. Electroanal. Chem.* **1982**, *131*, 381.

(15) Compion, A.; Mullins, D. R. *Chem. Phys. Lett.* **1983**, *94*, 576.

(16) Yamada, H.; Tani, N.; Yamamoto, Y. *J. Electron Spectrosc. Relat. Phenom.* **1983**, *30*, 13.

(17) (a) Gao, J. S.; Tian, Z. Q. *Chem. Phys. Lett.* **1996**, *262*, 151. (b) Tian, Z. Q.; Ren, B.; Wu, D. Y. *J. Phys. Chem. B* **2002**, *106*, 9463.

(18) Brolo, A. G.; Irish, D. E.; Lipkoski, J. *J. Phys. Chem. B* **1997**, *101*, 3906.

(19) Nicholson, M. A.; Aust, J. F.; Booksh, K. S.; Bell, W. C.; Myrick, M. L. *Vib. Spectrosco.* **2000**, *24*, 157.

(20) Muniz-Miranda M. *Chem. Phys. Lett.* **2001**, *340*, 437.

(21) Haq, S.; King, D. A. *J. Phys. Chem.* **1996**, *100*, 16957.

(22) Ikezawa, Y.; Sawatari, T.; Terashima, H. *Electrochim. Acta* **2001**, *46*, 1333.

(23) Nanbu, N.; Kitamura, F.; Ohsaka, T.; Tokuda, K. *J. Electroanal. Chem.* **1999**, *470*, 136.

(24) Cai, W. B.; Wan, L. J.; Noda, H.; Hibino, Y.; Ataka, K.; Osawa, M. *Langmuir* **1998**, *14*, 6992.

(25) Anderson, M. P.; Uvdal, P. *J. Phys. Chem. B* **2001**, *105*, 9458.

(26) Bader, M.; Haase, J.; Frank, K. H.; Puschmann, A.; Otto, A. *Phys. Rev. Lett.* **1986**, *56*, 1921.

(27) Giessel, T.; Schaff, O.; Lindsay, R.; Baumagartel, P.; Polcik, M.; Bradshaw, A. M.; Koebbel, A.; McCabe, T.; Bridge, M.; Lloyd, D. R.; Woodruff, D. P. *J. Chem. Phys.* **1999**, *110*, 9666.

(28) Creighton, J. A.; Alvarez, M. S.; Weltz, D. A.; Garoff, S.; Klm, M. W. *J. Phys. Chem.* **1983**, *87*, 4793.

(29) Moskovits, M. *Chem. Phys. Lett.* **1983**, *98*, 498.

(30) Mizutani, G.; Ushioda, S. *J. Chem. Phys.* **1989**, *91*, 598.

(31) (a) Wu, D. Y.; Ren, B.; Jiang, Y. X.; Xu, X.; Tian, Z. Q. *J. Phys. Chem. A* **2002**, *106*, 9042. (b) Wu, D. Y.; Ren, B.; Xu, X.; Liu, G. K.; Yang, Z. L.; Tian, Z. Q. *J. Chem. Phys.* **2003**, *119*, 1701.

(32) Wu, D. Y.; Hayashi, M.; Chang, C. H.; Liang, K. K.; Lin, S. H. *J. Chem. Phys.* **2003**, *118*, 4073.

(33) (a) Frisch, M. J.; Trucks, G. W.; Schlegel, H. B.; Gill, P. M. W.; Johnson, B. G.; Robb, M. A.; Cheeseman, J. R.; Keith, T. A.; Petersson, G. A.; Montgomery, J. A.; Raghavachari, K.; Al-Laham, M. A.; Zakrzewski, V. G.; Ortiz, J. V.; Foresman, J. B.; Cioslowski, J.; Stefanov, B. B.; Nanayakkara, A.; Challacombe, M.; Peng, C. Y.; Ayala, P. Y.; Chen, W.; Wong, M. W.; Andres, J. L.; Replogle, E. S.; Gomperts, R.; Martin, R. L.; Fox, D. J.; Binkley, J. S.; Defrees, D. J.; Baker, J.; Stewart, J. P.; Head-Gordon, M.; Gonzales, C.; Pople, J. A. *Gaussian 98*; Gaussian Inc.: Pittsburgh, PA, 1998. (b) Legge, F. S.; Nyberg, G. L.; Peel, J. B. *J. Phys. Chem. A* **2001**, *105*, 7905. (c) de Oliveira, G.; Martin, J. M. L.; de Proft, F.; Geerlings, P. *Phys. Rev. A* **1999**, *60*, 1034. (d) Alcami, M.; Gonzalez, A. I.; Mo, O.; Yanez, M. *Chem. Phys. Lett.* **1999**, *307*, 244.

(34) (a) Hay, P. J.; Wadt, W. R. *J. Chem. Phys.* **1985**, *82*, 270. (b) Wadt, W. R.; Hay, P. J. *J. Chem. Phys.* **1985**, *82*, 284. (c) Hay, P. J.; Wadt, W. R. *J. Chem. Phys.* **1985**, *82*, 299.

(35) (a) Pulay, P.; Fogarasi, G.; Pang, F.; Boggs, J. E. *J. Am. Chem. Soc.* **1979**, *101*, 2550. (b) Fogarasi, G.; Zhou, X.; Taylor, P. W.; Pulay, P. *J. Am. Chem. Soc.* **1992**, *114*, 8191.

(36) Wiberg, K. B.; Walters, V. A.; Wong, K. N.; Colson, S. D. *J. Phys. Chem.* **1984**, *88*, 6067.

(37) Xue, Y.; Xie, D.; Yan G. *Int. J. Quantum Chem.* **2000**, *76*, 686.

(38) Wilson, E. B.; Decius, J. C.; Cross, P. C. *Molecular Vibration*; McGraw-Hill: New York, 1955.

(39) Califano, S. *Vibrational States*; John Wiley & Sons: London, 1976.

(40) Herzberg, G. *Molecular Spectra and Molecular Structure: II. Infrared and Raman Spectra of Polyatomic Molecules*; Van Nostrand Reinhold Co.: New York, 1945.

(41) El-Azhary, A. A.; Suter, H. U. *J. Phys. Chem.* **1996**, *100*, 15056.

(42) Lombardi, J. R.; Davis, B. *Chem. Rev.* **2002**, *102*, 2431, and references therein.

(43) Pyykkö, P. *Angew. Chem., Int. Ed.* **2002**, *41*, 3573.

(44) Fournier, R. *J. Chem. Phys.* **2001**, *115*, 2165.

(45) Jug, K.; Zimmermann, B.; Calaminici, P.; Koster, A. M. *J. Chem. Phys.* **2002**, *116*, 4497.

(46) Mills, G.; Gordon, M. S.; Metiu, H. *Chem. Phys. Lett.* **2002**, *359*, 493.

(47) Bilic, A.; Reimers, J. R.; Hush, N. S. *J. Phys. Chem. B* **2002**, *106*, 6740.
(48) Boussard, P. J. E.; Siegbahn, P. E.; Svensson, M. *Chem. Phys. Lett.* **1994**, *231*, 337.
(49) Mitchell, S. A.; Lian, L.; Rayner, D. M.; Hackett, P. A. *J. Phys. Chem.* **1996**, *100*, 15708.
(50) Tevault, D. E.; Smardzewski, R. R. *J. Chem. Phys.* **1982**, *77*, 2221.
(51) Krasser, W.; Kettler, U.; Bechthold, P. S. *Chem. Phys. Lett.* **1982**, *86*, 223.
(52) Lee, J. G.; Ahner, J.; Yates, J. T., Jr. *J. Chem. Phys.* **2001**, *114*, 1414.
(53) Yang, M. C.; Rockey, T. J.; Pursell, D.; Dai, H. L. *J. Phys. Chem. B* **2001**, *105*, 11945.
(54) Lipkowski, J.; Stolberg, L. In *Adsorption of Molecules at Metal Electrodes*; Lipkowski, J., Ross, P. N., Eds.; VCH: New York, 1992; p 171.
(55) Pongor, G.; Fogarasi, G.; Boggs, J. E.; Pulay, P. *J. Mol. Spectrosc.* **1985**, *114*, 445.
(56) Arenas, J. F.; Tocon, I. L.; Otero, J. C.; Marcos, J. I. *J. Mol. Struct.* **1999**, *476*, 139.
(57) Yang, W.-H.; Schatz, G. C. *J. Chem. Phys.* **1992**, *97*, 3831.
(58) Destexhe, A.; Smets, J.; Adamowicz, L.; Maes, G. *J. Phys. Chem.* **1994**, *98*, 1506.
(59) Martin, J. M. L.; Alsenoy, C. V. *J. Phys. Chem.* **1996**, *100*, 6973.
(60) Dkhissi, A.; Adamowicz, L.; Maes, G. *J. Phys. Chem. A* **2000**, *104*, 2112.
(61) Akyüz, S.; Dempster, A. B.; Morehouse, R. L.; Suzuki, S. *J. Mol. Struct.* **1973**, *17*, 105.
(62) Osawa, M. In *Near-Field Optics and Surface Plasmon Polaritons*; Springer: Berlin, 2001; p 163.
(63) Kreyenschmidt, M.; Eysel, H. H.; Asthana, B. P. *J. Raman Spectrosc.* **1993**, *24*, 645.
(64) Clark, R. J. H.; Willams, C. S. *Inorg. Chem.* **1965**, *4*, 350.
(65) Ferwerda, R.; van der Maas, J. H.; van Duijneveldt, F. B. *J. Mol. Catal. A* **1996**, *104*, 319.
(66) Cheng, P. Y.; Duncan, M. A. *Chem. Phys. Lett.* **1988**, *152*, 341.
(67) Wallimann, F.; Frey, H.; Leutwyler, S.; Riley, M. *Z. Phys. D* **1997**, *40*, 30.